Vietnam Journal of Earth Sciences, 43(3), 316-322, https://doi.org/10.15625/2615-9783/16198

Vietnam Academy of Science and Technology
Vietnam Journal of Earth Sciences
http://www.vjs.ac.vn/index.php/jse

Late pleistocene movement of Nam O-Nam Dong fault: evidence from electron spin resonance dating of fault gouge in the Western Da Nang city

Nguyen Quoc Hung, Tran Thanh Hai, Vu Anh Dao, Ngo Xuan Thanh*

Hanoi University of Mining and Geology, Hanoi, Vietnam

Received 15 July 2020; Received in revised form 21 June 2021; Accepted 25 July 2021

ABSTRACT

The Nam O-Nam Dong fault is rated as one of the most seismic source zones in Central Vietnam. Field investigation in the mountainous areas in the Cam Le and Hoa Vang districts (Da Nang city), which is a part of the Nam O-Nam Dong fault zone, the authors have discovered fault gouge zone of 5-40 cm width within the Dai Loc granitic rock. Two fault gouge samples were collected for Electron Spin Resonance (ESR) dating. The results from the ESR dating on the quartz grains from the fault gouge samples showed the youngest age from the smallest fraction, probably indicating that ESR signals in the fractions were completely zeroed at the time of faulting due to frictional heat. The preliminary results from the ESR dating on the quartz grains from the fault gouge samples indicate the existence of faulting events from 15.05±3.55 ka to 18.21±4.06 ka ago. Multiple actives during the late Pleistocene - Holocene of this fault had uplifted the fault gouge from a depth-seated to the present-day locality. These data suggest that this fault zone can be classified as a potentially active fault zone and presents some seismic hazards.

Keywords: Quartz ESR dating, active fault, central Vietnam, Indochina.

1. Introduction

Ikeya et al. (1982) showed that radiation-sensitive ESR signals in quartz from the fault gouge exhibit equivalent doses which are much less than saturation or steady-state doses observed in adjacent, unfaulted host rocks. Since his work, various researchers have recognized that complete resetting of ESR signals will only occur when the faulted material has been subject to some normal stress at the time of faulting, and when there has been sufficient displacement during the faulting event (e.g. Ariyama, 1985; Lee and Schwarcz, 1994). From the detailed investigation of the ESR age of known fault through stratigraphic relationship, Ito and Sawada (1985) suggested that the rocks must be buried at a minimum depth of 20 m for reverse faults, 70 m for strike-slip faults, and 100 m for normal faults in order to assure adequate normal stress for resetting the ESR signals at the time of fault movement. Grun (1992) described that the sample must have been at a depth of at least 250 m for complete resetting of ESR signals. Lee and Schwarcz (1994) have refined the

*Corresponding author, Email: ngoxuanthanh@humg.edu.vn

criteria for complete zeroing of ESR signals at the time of fault movement and suggested that the depth of fault rocks at the time of reactivation can be estimated from uplift rate and the ESR age.

The basic principle of dating by ESR spectroscopy is the detection of paramagnetic centers and free radicals in solids and fluids. Therefore, the basic assumption for ESR dating is that the samples do not contain paramagnetic centers at t = 0 (Ikeya et al., 1982, and references therein). If samples had previously acquired paramagnetic centers, a geological event at t = 0 has to completely destroy these centers (Grun, 1992). Its application for dating fault movement is based on the assumption that the lattice defects produced by natural radiation in quartz grains are annihilated around the fault plane at the time of fault formation or movement by the high shearing stresses and raised temperatures, by zeroing of the ESR signals (Lee & Schwarcz, 1993).

In this study, the authors investigated fault zones in the western Da Nang city, Central Vietnam, where the Nam O-Nam Dong fault cut through different rock type (Fig. 1a). The study area is composed of Paleozoic meta-sedimentary and intrusive rocks in the west, and late Quaternary sediment in the east (Fig. 1b). The A Vuong and Long Dai formations are composed of weakly metamorphosed quartz-muscovite-sericite schist, siliceous schist, felsic effusive, banded dolomitic marble, actinolite-epidote schist, and black shale, and preferred as forming during Ordovician (Tran and Vu., 2011). The Dai Loc and Hai Van S-type granites that intruded into the A Vuong Formation yielded ages ca. 427-406 Ma and 230-240 Ma, respectively (Carter et al., 2001; Thanh et al., 2014; 2016; Nguyen et al., 2020). The Dai Loc granite with mylonitic texture is composed of porphyrite plagioclase, quartz, K-feldspar, biotite, and muscovite, representing S-type granite formed by crust thickening during the collision of Kon Tum and Truong Son terranes. In the east, the area consists of mainly Quaternary sediment that formed along the Eas Vietnam Sea coast, alternating conglomerate, sand, and silt sediments unconformably deposited on the Paleozoic rocks. Holocene sediment is distributed along with the present-day river systems and near the coast (Tran and Vu, 2011).

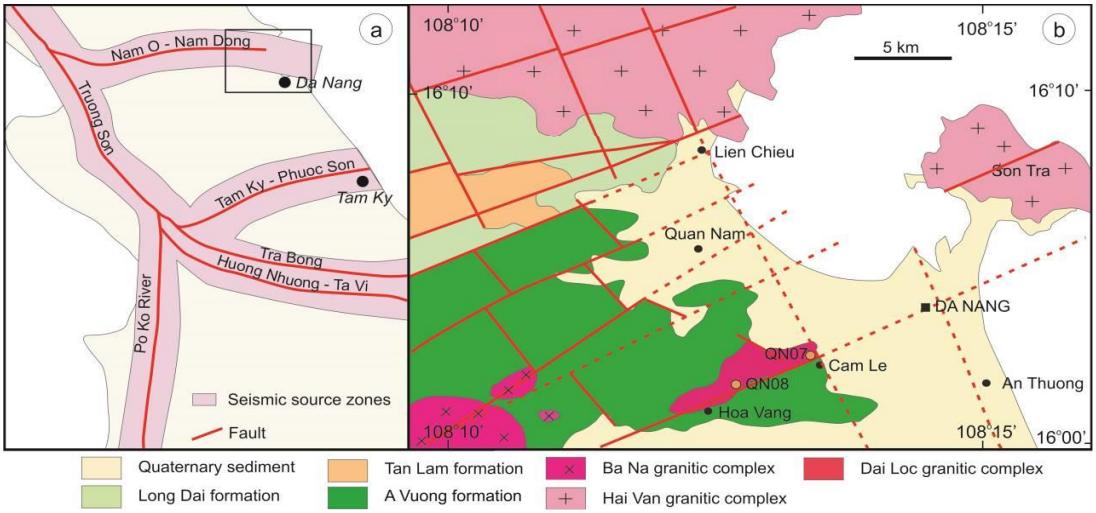

Figure 1. (a) Map of the seismic sources in Central Vietnam (Nguyen, 2014, and Nguyen et al., 2016). (b) Geological map of the Da Nang area (Modified from Nguyen, 1995) showing sample localities

The Nam O-Nam Dong fault is extended from NW Quang Nam province through Da Nang city to the East Vietnam Sea. The fault cuts the Paleozoic rocks, forming fault gouges about 5-40 cm thick. Nguyen et al. (2016) reported earthquakes of 4-4.9 magnitude in the fault zone that probably suggesting active fault results. Additionally, the previous studies on remote sensing, fault rupture, geomorphology, hot spring, Rn, Hg, CH_4 gasses have also supported evidence of active faults (e.g. Nguyen, 2004; Nguyen and Pham, 2014; Nguyen et al., 2016). Although the fault is classified as one of the highest seismic potential zones in Central Vietnam (Ngo et al., 2008, 2017; Nguyen et al., 2016), there is no direct age data from the fault zone has been analyzed. In this paper, the authors investigated fault systems in the northwestern Quang Nam province and collected two fault gouge samples of the NE-SW fault system for quartz ESR age dating (Fig. 1b).

2. Sample preparation and analytical methods

Sample collection

Field research works were carried out on a mountainside in the Cam Le and Hoa Vang areas, Da Nang city. The authors recognized a fault system striking consistently from ~N45°E to ~N60°E, dipping 70°-80° to NW. The fault system has commonly fault gouges zones of 3-40 cm width. Slickensides observed on fault scarps suggest the feature of both dextral and normal fault. Two gouge samples were collected from rock quarries in the Cam Le (QN07) and Hoa Vang (QN08) districts (Da Nang). The samples were collected from about a 1 cm width zone near the boundary between the fault gouge and fault wall rocks (Fig. 2b). Before collecting the samples, the outcrops were dug about 100 cm from the surface to avoid effects from weathering and surface water. The fault gouge samples were stored in plastic bags to avoid any loss of water as well as contamination.

Figure 2. Outcrop photos showing fault gouge zone formed along with the NE-SW fault system in the W Da Nang city. (a) Outcrop of the sample QN07 showing dextral-normal fault scarp cut through the mylonitic Dai Loc granite, and (b) Outcrop showing fault gouge zone of the sample QN08

Sample preparation

Prior to ESR analysis, the gouge samples were washed with distilled water and then dried in a dark environment to avoid possible effects of sunlight on the ESR signal intensity (Ikeya et al., 1982). The dried samples were sieved to take the fractions of 0.5-1 mm. Magnetic minerals were removed using a magnetic separator. The sieved samples were treated with 6N hydrochloric acid (HCl)

overnight, and then with a 1% HF and 1% HNO_3 mixture for 12 h, prior to heavy liquid (sodium polytungstate solution) separation. The quartz grains were etched with 46% HF for 1 h to dissolve any contaminating feldspar and then treated with 6N HCl overnight. Finally, the samples were re-sieved into the fractions of 75-125 μm, 45-75 μm, and <45 μm.

Gamma-ray irradiation and ESR measurement

The ESR dose-response curves of quartz grains from impurity centers are known to grow with high radiation doses (Yokoyama et al., 1985). Therefore, we used the dose-saturated ESR signal intensities. To obtain the additive dose responses of the signals, subsamples of quartz samples R2, R3, and S4 were divided into 6-9 aliquots. They were then irradiated using a ^{60}Co gamma-ray source with doses ranging from 0.2 to 3 kGy and a dose rate of 100 Gy/h at the Takasaki Research Institute of the Japan Atomic Energy Agency. Based on the results from these irradiated samples, all samples were irradiated to a dose.

ESR measurements were conducted using a JESX320 X-band spectrometer (JEOL RESONANCE Inc.) with the Liquid Helium Variable Temperature System (ES-CT470). The Al center signals from the quartz samples were measured at 77 K (-196°C) using a microwave power of 5 mW, a sweep time of 2 min, a time constant of 0.03 s, an amplitude of field modulation of 0.1 mT, and a modulation frequency of 100 kHz. Fig. 2 shows the ESR spectrum of the study samples at 77 K. We took the relative height from the top of the first peak to the bottom of the 16th peak of the main hyperfine structures as the Al center intensity (Yokoyama et al., 1985; Toyoda and Falguères, 2003; Shimada and Toyoda, 2004). Given that the proxy center signal at g = 2.067 overlaps the Al center signal, Toyoda and Falguères (2003) and Toyoda, 2015 suggested taking the peak height between g = 2.018 and 1.993 as the Al center signal intensity to avoid the contribution from the proxy center signal. To calculate the g values of the ESR signals and to further check the sensitivity of the ESR spectrometer, we used the intensity of a standard MnO marker inside the cavity. Each sample was measured five times, and the sample tube was rotated in the cavity to average the angular dependence of the ESR signals. For normalization and sensitivity correction, the average peak intensities were divided by the weight of the sample and by the standard MnO marker signal intensity, which was measured together with the sample.

4. Results and discussion

The natural and g-irradiated ESR spectra of quartz grains derived from the fault gouge are shown in Fig. 3. The results of ESR analysis of the two samples show consistent ESR ages for Al signals (Fig. 3 Table 1). As the Al and E' centers are more unstable than other centers (Stapelbroek et al., 1979; Shimokawa et al., 1984; Isoya et al., 1983; Imai et al., 1985), they were widely used in fault gouge dating (e.g., Fukuchi & Imai, 1998; Yin et al., 2002; Ulusoy, 2004; Lee & Yang, 2007). The plot of ESR ages vs. grain sizes is shown in Fig. 4.

Previous studies have tested of zeroing of ESR signals, the normal stress and shear strain (displacement) needed for complete resetting during fault movement. Fig. 4 show that the ESR ages (Al centers) get younger towards smaller size fraction, which possibly indicates a complete resetting at the time of fault movements for the smallest fractions (Tanner and Brandes, 2019). The youngest ages of samples QN07 (15.05±3.55 ka) and QN08 (18.21±4.60 ka) obtained from the smallest sample factions (<45 μm) (Table 1) suggest late Pleistocene fault activity (Fig. 4, 5 and Table 1).

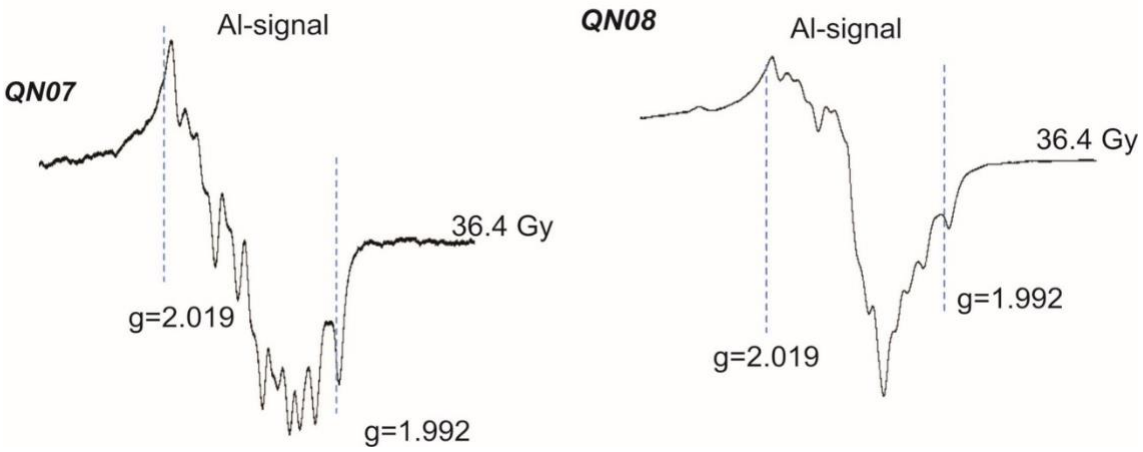

Figure 3. ESR powder spectrums of quartz in faults gouge at 77 K showing the signals of the Al-centers for the study samples

Table 1. ESR analytical data and results for samples QN07 and QN08

Sample	Fraction (μm)	DE (Gy)	Dose rate (μGy/y)	ESR Age (ka)
QN07	<45	141.05±31.33	9.4	15.05±3.55
	45-75	178.26±63.65	8.74	20.40±5.29
	75-125	201.80±52.65	8.54	22.59±6.30
QN08	0-45	203.54±58.07	11.18	18.21±4.60
	45-75	270.95±94.46	10.14	26.72±6.23
	75-125	336.38±253.75	9.57	35.15±12.50

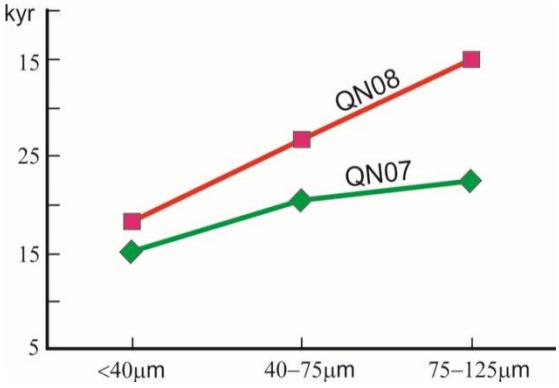

Figure 4. Al signal ages VS. grain sizes of the study samples

Active fault can be defined as a fault that will soon cause another earthquake (e.g., historical, Holocene, or Quaternary). Geologists generally believe faults to be active when there has been evidence of some seismic activities or some movements observed in the past 11,000 years (during Holocene). The youngest ages recorded in the samples of this study indicate multiple active phases of the faults systems occurring during the late Pleistocene (ranging from 15.05±3.55 ka to 18.21±4.60 ka). The fault gouge cannot be generated along faults in unconsolidated sediments due to low confining stress near the surface. Additionally, the locality near the surface will not create high stress and temperature for ESR zeroing. It follows that the ESR signal will not record the very young movement of the fault. The fault gouge presently exposed at the surface was formed at a certain depth underground and subsequently brought to the surface through crustal uplift. According to Carter et al. (2001), average regional denudation in East Asia occurred at a similar rate of ~40±10 m/Myr since c. 16 Ma ago. Therefore, we consider that this gouge has

been moved up along the fault zone to the present-day sites by the multiple activities of the faults during the Late Pleistocene-Holocene. Nguyen et al. (2019) also reported Holocene ESR-ages of NE-SW faults in the Duy Xuyen District of Quang Nam province. Additionally, based on seismic data recorded from over 58 earthquakes during 1903 to 2014 years in the Quang Nam area, Nguyen et al. (2016) suggest that the earthquakes in the Quang Nam region occurred correlated to the movements of the Tam Ky-Phuoc Son, Tra Bong, and Da Nang-Nam Dong (also termed as Nam O- Nam Dong) fault systems.

5. Conclusions

The ESR ages of the Da Nang-Nam Dong fault zone appear to be clustered into active and rest periods. The fault rocks developed in this fault zone are reactivated at least during the late Pleistocene. During the late Pleistocene-Holocene of this fault, multiple actives had uplifted the fault gouge from depth-seated to the present-day locality. These data suggest that this fault zone can be classified as a potentially active fault zone (Keller and Pinter, 1996) and presents some seismic hazards to the nuclear power plant close to this fault zone.

Acknowledgments

This research was performed for the Research Project number KC.09.30/16-20 funded by the Ministry of Science and Technology of Vietnam. We thank Prof. Shin Toyoda (Okayama University of Science) for supporting and guiding the ESR analyses.

References

Ariyama T., 1985. Conditions of resetting the ESR clock during faulting. In: Ikeya, M., Miki, T. (Eds.), ESR Dating and Dosimetry, Ionics, 251-258.

Fukuchi T., Imai N., 1998. Resetting experiment of E′ centers by natural faulting - the case of the Nojima earthquake fault in Japan. Quaternary Science Reviews, 17(11), 1063-1068.

Grün R., 1992. Remarks on ESR dating of fault movements. Journal of the Geological Society, 149(2), 261-264.

Ikeya M., Miki N., Tanaka K., 1982. Dating of fault by electron spin resonance on intrafault materials, Science, 215, 1392-1393.

Imai N., Shimokawa K., Hirota M., 1985. ESR dating of volcanic ash. Nature, 314(6006), 81-83.

Isoya J., Bowman M.K., Norris J.R., Weil J.A., 1983. An elcetron spin echo envelope modulation study of lithium hyperfine and quadropole coupling in the A(Ti-Li) center of α-quartz. Journal of Chemical Physics, 78(4), 1735-1746.

Ito T., Sawada S., 1985. Reliable criteria for selection of sampling points for ESR fault dating. ESR Dating & Dosimetry, Ionics, Tokyo, 229-237.

Keller E.D., Pinter N., 1996. Active Tectonics: Earthquakes, Uplift, and Landscape. Prentice-Hall, New Jersey.

Lee H.K., Schwarcz H.P., 1994. Criteria for complete zeroing of ESR signals during faulting of the San Gabriel fault zone, S. California; Tectonophysics, 235, 317-337.

Lee H.K., Yang J.S., 2007. ESR dating of the Eupchon fault, South Korea. Quaternary Geochronology, 2, 392-397.

Ngo L.T., Rodkin M.V., Tran V.P, Nguyen Q. Phung, Vu T.H., 2017. Assessment of earthquake hazard for the northwestern Vietnam from geological and geophysical data using an original program package. Journal of Volcanology and Seismology, 11, 164-171.

Ngo T.D., Nguyen M.D., Nguyen D.B., 2008. A review of the Current Vietnamese Earthquake Design Code. EJSE Special Issue, 32-41.

Nguyen H.N., Pham T.T., Nguyen T.N., 2016. Probabilistic seismic hazard assessment for the Tranh River hydropower plant No 2 site, Quang Nam province. Vietnam Journal of Earth Sciences, 38(2), 189-203.

Nguyen H.P., 2004. Seismic Hazard Maps of Vietnam and the East Vietnam Sea. Journal of Earth's Sciences, 26(2), 97-111 (in Vietnamese).

Nguyen Q.H., Ngo X.T., Vu A.D., 2020. U-Pb ages of zircon from I- and S-type granites from northern

Kon Tum terrane: Implications for late Paleozoic-Mesozoic magmatism in Central Vietnam. Journal of the Geological Society of Korea, 56(6), 727-735.

Nguyen Q.H., Vu A.D., Ngo X.T., Tran T.H., Dang V.B., 2019. ESR dating of fault gouge in the midstream Thu Bon River: New evidence of fault movements during late Pleistocene-Holocene. Geology Journal, 367pp (in Vietnamese with English abstract).

Nguyen V.T. (edt.), 1995. Geological and Mineral Resources map sheet D-49-I on scale 1:200,000. Geological Survey of Vietnam, Hanoi.

Shimada A., Toyoda S., 2004. The optimal conditions of microwave and temperature of ESR measurement suitable for impurities centers in quartz. Advances in ESR Applications, 21, 13-16.

Stapelbroek M., Griscom D.L., Friebele E.J., Sigel G.H., 1979. Oxygen associated trapped holecenters in high purity fused silicas. J. Non-Cryst. Solids, 32, 313-326.

Tanner D., Brandes C., 2019. Understanding Faults. Chapter 7. Elsevier, 380pp.

Thanh N.X., Hai T.T., Hoang N., Vu Q.L., Kwon S.H., Itaya T., Santosh M., 2014. Backarc mafic-ultramafic magmatism in Northeastern Vietnam and its regional tectonic significance. Journal of Asian Earth Sciences, 90, 45-60.

Thanh N.X., Santosh M., Tran T.H., Pham T.H., 2016. Subduction initiation of Indochina and South China blocks: insight from the forearcophiolitic peridotites of the Song Ma Suture Zone in Vietnam. Geological Journal, 51(3), 421-442.

Toyoda S., 2015. Paramagnetic lattice defects in quartz for applications to ESR dating. Quaternary Geochronology, 30, 498-505.

Toyoda S., Falgueres C., 2003. The method to represent the ESR signal intensity of the aluminum hole center in quartz for the purpose of dating. Adv. ESR Appl., 20, 7-10.

Toyoda S., Hattori M., 2000. Formation and decay of the E1’ center and of its precursor. Applied Radiation Isotopes, 52, 1351-1356.

Toyoda S., Schwarcz H.P., 1997b. The hazard of the Counterfeit E1' signal in quartz to ESR dating of fault movements. Quat. Sci. Rev. (Quat. Geochronol.), 16, 483-486.

Ulusoy Ü., 2004. ESR dating of North Anatolian (Turkey) and Nojima (Japan) faults. Quaternary Science Reviews, 23(1-2), 161-174.

Yin G.M., Lu Y.C., Wei L.Y., Zhang J.Z., 2002. Chronological study of faulting events of Gaoliying fault, Beijing. Seismology and Geology, 24(1), 101-110.

Yokoyama Y., Falgueres C., Quaegebeur J.P., 1985. ESR dating of quartz from quaternary sediments: first attempt. Nucl. Tracks Radiat. Meas., 10, 921-928.